Parts-Per-Billion Fourier Transform Ion Cyclotron Resonance Mass Measurement Accuracy with a "Walking" Calibration Equation

ARTICLE *in* ANALYTICAL CHEMISTRY · MARCH 2011

Impact Factor: 5.64 · DOI: 10.1021/ac102943z · Source: PubMed

8 AUTHORS, INCLUDING:

Amy M. Mckenna
Florida State University
54 PUBLICATIONS **980** CITATIONS
SEE PROFILE

Greg Blakney
National High Magnetic Field Laboratory
23 PUBLICATIONS **703** CITATIONS
SEE PROFILE

analytical chemistry

ARTICLE

pubs.acs.org/ac

Parts-Per-Billion Fourier Transform Ion Cyclotron Resonance Mass Measurement Accuracy with a "Walking" Calibration Equation

Joshua J. Savory,[†] Nathan K. Kaiser,[†] Amy M. McKenna,[†] Feng Xian,[‡] Greg T. Blakney,[†] Ryan P. Rodgers,[†,‡] Christopher L. Hendrickson,[*,†,‡] and Alan G. Marshall[*,†,‡]

[†]National High Magnetic Field Laboratory, Florida State University, 1800 East Paul Dirac Drive, Tallahassee, Florida 32310-4005, United States

[‡]Department of Chemistry, Florida State University, 95 Chieftain Way, Tallahassee, Florida 32306, United States

ABSTRACT: Ion cyclotron resonance frequency, f, is conventionally converted to ion mass-to-charge ratio, m/z (mass "calibration") by fitting experimental data spanning the entire detected m/z range to the relation, $m/z = A/f + B/f^2$, to yield rms mass error as low as ~200 ppb for ~10 000 resolved components of a petroleum crude oil. Analysis of residual error versus m/z and peak abundance reveals that systematic errors limit mass accuracy and thus the confidence in elemental composition assignments. Here, we present a calibration procedure in which the spectrum is divided into dozens of adjoining segments, and a separate calibration is applied to each, thereby eliminating systematic error with respect to m/z. Further, incorporation of a third term in the calibration equation that is proportional to the magnitude of each detected peak minimizes systematic error with respect to ion abundance. Finally, absorption-mode data analysis increases mass measurement accuracy only after minimization of systematic errors. We are able to increase the number of assigned peaks by as much as 25%, while reducing the rms mass error by as much as 3-fold, for significantly improved confidence in elemental composition assignment.

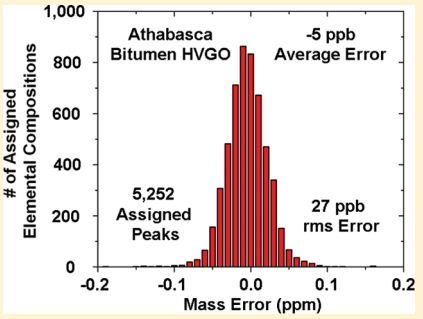

Devices similar to a Fourier transform ion cyclotron resonance (FTICR) mass spectrometer[1] are used by the physics community for mass measurement of single ions with precision as high as $m/\delta m = 10^{10}$.[2] Mass accuracy for a complex mixture (containing ions with up to thousands of different elemental compositions) is much lower because (a) the measurement spans a much wider cyclotron frequency range; (b) ions are typically excited to much larger ion cyclotron radius (at which the applied electrostatic, rf electric, and static magnetic fields exhibit greater deviation from ideal quadrupolar electrostatic, linear rf electric, and spatially homogeneous magnetic fields); (c) image charge from the surrounding electrodes shifts the resonances; (d) presence and variation in relative abundance of ions of different mass-to-charge ratio, m/z; and (e) variation in number of trapped ions from one time-domain data acquisition to the next, if repeated acquisitions are averaged to improve the signal-to-noise ratio. Thus, systematic error can significantly exceed random error.

Typically, observed ICR frequency is converted to m/z by means of a two term equation:[3,4]

$$m/z = A/f + B/f^2 \quad (1)$$

Equation 1 neglects image charge[5,6] and relativistic frequency shifts[7] and is based on a perfectly homogeneous magnetic field and a purely quadrupolar (i.e., quadratic in radius) electrostatic potential arising from the applied trapping potential plus the space charge potential from all trapped ions. A method to account for variation in the total ion abundance in the ICR cell has been described by Easterling et al.,[8] based on the pioneering work of Jeffries et al.[9] For simple mixtures, the effectiveness of several different calibration laws that formally account for space charge effects and were able to achieve low part per million (ppm) mass accuracy has previously been evaluated.[10] More recently, the same calibration laws were applied to FTICR MS with automatic gain control[11] to extend the dynamic range of the instrument and maintain subppm mass accuracy.[12] So-called calibrant-free techniques have also been developed to account for space-charge induced frequency shifts in spectra which contain multiple charge states of the same molecular species (DeCAL)[13] or neighboring fragment ions of a known mass difference (COFI).[14]

The shift in ICR frequency of ions of a given m/z, due to ions of all other m/z, can be modeled by treating the ions of other m/z as a ring of charge at the same ICR radius, leading to eq 2, in which I represents the abundance of the m/z species in eq 2.[15,16]

$$m/z = A/f + B/f^2 + CI/f^2 \quad (2)$$

To account for frequency shifts caused by the interaction of ion clouds at different radii[17] and negative frequency peaks in combination with collision damping,[18] additional terms can be incorporated into eq 1.

Received: November 9, 2010
Accepted: January 7, 2011
Published: January 28, 2011

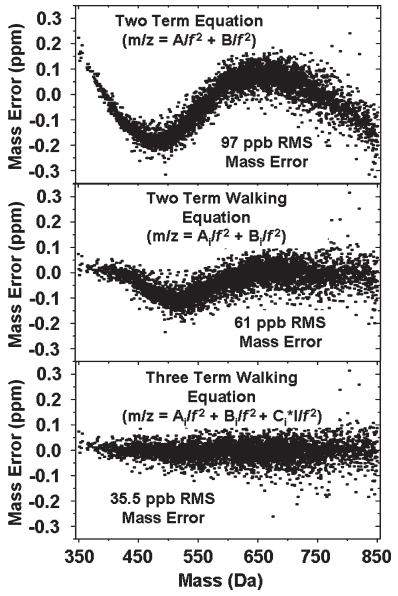

Figure 1. Mass error (rms) for all 5 252 electrosprayed negative-ion 9.4 T FTICR magnitude-mode mass spectral peaks from an Athabasca bitumen heavy vacuum gas oil (HVGO) distillate calibrated with the conventional two term eq 1 (top), along with subsequent recalibration of the same data with either the two term walking calibration of eq 3 (middle) or a three term walking calibration with an abundance-dependent term of eq 4 (bottom). In total, 31 calibration segments were used for both the two and three term walking calibrations.

Calibration of spectra in discrete m/z ranges to deal with unknown sources of m/z-dependent systematic error has previously been proposed and implemented. Rodgers et al. performed separate internal calibrations for a low (m/z 90−185) and high (m/z 185−300) mass region for a crude oil mass analysis.[19] Subsequently, a robust calibration method improved proteomics mass analysis in which individual peaks are calibrated with different parameters based on their m/z region, elution time, ion abundance, and total ion abundance.[20] Here, we present a "walking" calibration equation that has proved strikingly successful in virtually eliminating m/z-dependent systematic error from broadband mass spectra. As explained below, we apply the two-term mass calibration separately to each of up to 31 adjoining segments of a broadband absorption-mode FTICR mass spectrum to yield routine sub-100 ppb mass measurement for petroleum crude oil samples with >10 000 peaks in a single FTICR mass spectrum. Further, we incorporate eq 2 in each segment to minimize systematic error with respect to ion abundance. Finally, absorption-mode data analysis increases mass measurement accuracy but only after minimization of systematic error. We are able to increase the number of assigned peaks by as much as 25%, while reducing the rms mass error by as much as 3-fold, for significantly improved confidence in elemental composition assignment.

EXPERIMENTAL SECTION

Sample Preparation. Stock solutions of either a distillate fraction (500−538 °C) from an Athabasca bitumen heavy vacuum gas oil (HVGO) or a North American crude oil were dissolved in 50:50 (v/v) toluene:methanol to a final concentration of 1 mg/mL. Each sample was further diluted to 0.25 mg/mL with 50:50 (v/v) toluene:methanol and 1% ammonium hydroxide or tetramethylammonium hydroxide solution to facilitate deprotonation during electrospray ionization.

Mass Analysis. Mass spectra were acquired with a custom-built 9.4 T FTICR mass spectrometer[21] at the National High Magnetic Field Laboratory in Tallahassee, FL. Negative ions were generated by electrospray ionization.[22] ICR time-domain transients were collected from a 7 segment open cylindrical cell with capacitively coupled excitation electrodes similar to the configuration of Tolmachev et al.[23] The 20−200 individual transients of 5.6 s collected for the HVGO and 100 individual transients of 6.1 s collected for the North American crude oil were averaged, apodized with a full-Hanning (magnitude spectrum) or half-Hanning (absorption spectrum[24]) weight function, and zero-filled once prior to fast Fourier transformation. For both samples, the achieved spectral resolving power approaches the theoretical limit[25] over the entire mass range, e.g., average resolving power at m/z 400 was approximately 1 000 000 in magnitude-mode and 1 650 000 in absorption-mode for the North American crude oil. Each m/z spectrum was internally calibrated with respect to an abundant homologous O_2 (HVGO) or N_1 (North American crude oil) series. To span the dynamic range required to calibrate a spectrum that includes an abundance-weighted term, the calibration data were expanded to include $^{13}C_1$ and $^{13}C_2$ isotopomers of the main monoisotopic homologous calibration series.

RESULTS AND DISCUSSION

Mass Spectral Segmentation: Walking Frequency-to-*m/z* Calibration Equation. Petroleum crude oil consists of many homologous series of species, each of whose members differ in elemental composition by integer multiples of CH_2, corresponding to 14.015 65 Da (or 14.000 00 Kendrick mass units).[26,27] Typically, a crude oil spectrum is internally calibrated from a single highly abundant series. Figure 1 (top) shows the mass error distribution as a function of m/z, resulting from the best fit of eq 1 to a single homologous series spanning the full m/z range. Although the mass errors are smaller than for any other mass analyzer, systematic variation in mass error across the m/z range is clearly evident. However, within a limited m/z segment (say ±10 Da), the mass error distribution is considerably narrower. We therefore divided the spectrum into N equal consecutive segments such that each segment contained at least three members of a homologous alkylation series (differing by multiples of CH_2). Each ith segment was then least-squares-fitted to a separate two term calibration (eq 3),

$$m/z = A_i/f + B_i/f^2 \quad (3)$$

with different A_i and B_i coefficients for each segment. We designate that stepwise procedure as a "walking calibration".

Optimization of the Calibration Segment Width. To remove a large and variable m/z-dependent systematic error, such as that in Figure 1 (top), the spectrum must be calibrated in relatively small segments (±10 Da). However, as the width of each calibration segment decreases, the number of internal calibrant peaks per segment also decreases, with a corresponding increase in random error in the calibration. Thus, the optimal calibration segment width will depend on both the m/z-dependent systematic error range and the signal-to-noise ratios of the calibrant peaks. We therefore plotted rms mass error for the full m/z range as a function of the m/z segment width in daltons (Figure 2) for the same Athabasca bitumen HVGO sample

dx.doi.org/10.1021/ac102943z |Anal. Chem. 2011, 83, 1732–1736

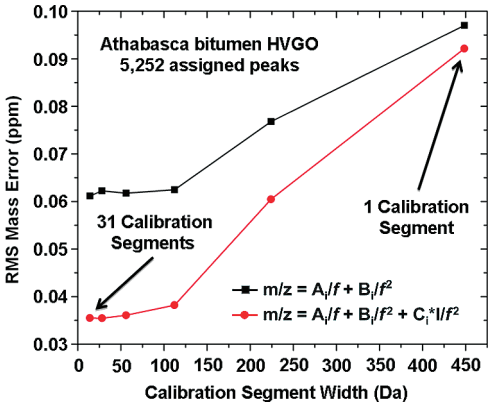

Figure 2. The rms mass error for calibration of the same time-domain data as for Figure 1 (top) but with either a walking two term calibration (eq 3, black) or three term walking equation with an abundance-dependent term (eq 4, red) as a function of the calibration segment width.

shown in Figure 1. Peak detection and mass assignment were initially performed with Predator analysis software.[28] To minimize the impact of random errors, the analysis was confined to peaks whose magnitude exceeded ~20σ of baseline noise. Furthermore, the spectrum was calibrated by use of the homologous series of the highest total abundance to achieve the highest precision. Recalibration was performed manually for each segment width with no subsequent peak reassignment. To improve the continuity of the full calibration for the smallest segment width (14.015 65 Da), three consecutive calibration masses spanning 28 Da were used to calculate A_i and B_i for each segment; the calibration data sets were overlapped by 14 Da, and the resultant calibrations were applied to the central 14 Da of the 28 Da range encompassed by the calibration data set.

Figure 2 shows that for either the two term or three term walking calibration, the overall rms error decreases with decreasing calibration segment width and the smallest rms error is reached at a 14 Kendrick mass unit segment. The improved mass measurement accuracy indicates that the error is primarily systematic, not random, as is expected if the series chosen for calibration is high in abundance relative to the other series.

Correction for *m/z*-Dependent Space Charge. Although recalibration of the single segment, two term (eq 1) calibration of Figure 1 (top) with a 31-segment, two term (eq 3) walking calibration (Figure 1 (middle)) reduces the overall rms mass error by ~37%, some systematic variation of mass error with m/z clearly remains, particularly in the range of m/z 450−650, namely, the spectral region exhibiting the highest dynamic range. We therefore performed a three term (eq 4) walking calibration. Inclusion of an abundance-dependent term and isotopomers ($^{13}C_1$ and $^{13}C_2$) of the main O_2 calibration series further reduces the total rms error by lowering the abundance-dependent systematic error (Figure 1, bottom). The dynamic range spanned by a given monoisotopic peak and its $^{13}C_2$ isotopomer varied from 20:1 to 5:1 as a function of carbon number. Additional coverage could be obtained through the inclusion of $^{13}C_3$ isotopomers but was not necessary for the calibration of this data.

$$m/z = A_i/f + B_i/f^2 + C_i I/f^2 \quad (4)$$

On the basis of these results, subsequent mass spectra were calibrated in segments with three masses per calibration segment for two term walking calibration and up to nine masses per calibration segment for three term calibration.

Table 1. Systematic and Random Error (After 200 Averaged Time-Domain Acquisitions) for the High Vacuum Gas Oil Data of Figure 1, with Different Calibration Equations[a]

	calibration equation	systematic error (ppb)	random error (ppb)
magnitude mode	$m/z = A/f + B/f^2$	91	31
	$m/z = A_i/f + B_i/f^2$	54	34
	$m/z = A_i/f + B_i/f^2 + IC_i/f^2$	18	32
absorption mode	$m/z = A/f + B/f^2$	107	16
	$m/z = A_i/f + B_i/f^2$	41	19
	$m/z = A_i/f + B_i/f^2 + IC_i/f^2$	25	15

[a] Results are shown for both absorption- and magnitude-mode analysis.

Error from Shot-to-Shot Variation in Total Trapped Ion Number. ICR frequency shifts downward (to a nearly m/z-independent extent) with increasing total number of trapped ions.[9] Thus, variation in the number of trapped ions from one time-domain data acquisition to the next will contribute additional mass measurement error. To minimize that error, we compute the sum of all above-threshold (6σ of baseline noise) mass spectral peak magnitudes for each acquisition but retain only those data sets whose summed peak heights fall within ±10% of a predefined total abundance until the desired number of (20−200) acquisitions is achieved. Thus, each averaged data set for an HVGO sample yielded an FTICR mass spectrum containing ~5 200 peaks at the 6σ threshold set by the lowest number of acquisitions (20).

Systematic vs Random Error. Systematic error may be determined from a fit of observed rms mass error as a function of the number of averaged scans to the theoretical error distribution of eq 5, in which N is the number of averaged acquisitions. Random error varies inversely with the square root of the number of averaged acquisitions, whereas systematic error is independent of the number of averaged acquisitions.[25]

$$\text{rms error} = \sqrt{[(\text{systematic error})^2 + (\text{random error}/\sqrt{N})^2]} \quad (5)$$

Table 1 lists the systematic and random errors, from 200 averaged time-domain signals, calculated from the same data presented in Figure 1. Two term walking calibration reduces the systematic error by a factor of ~2 for both magnitude- and absorption-mode spectra. Addition of an abundance-dependent term to the calibration equation reduces systematic error by another factor of ~2−3. Interestingly, random error was essentially independent of the choice of calibration equation but was ~2-fold lower for absorption-mode than magnitude-mode. For optimal calibration parameters, the total rms mass error decreased from 97 to 36 ppb for magnitude-mode and from 107 to 27 ppb for absorption-mode.

Number of Assigned Peaks. Encouraged by the results listed in Table 1, we automated the two term walking calibration procedure and incorporated it into our Predator analysis software. Table 2 lists the rms mass error and number of assigned peaks above 6σ of baseline noise for unsegmented and segmented two term automated calibration of electrosprayed negative

Table 2. Final Achieved rms Mass Error, Along with the Total Number of Peaks Detected and Assigned for Absorption-Mode (Phased) and Magnitude-Mode (Unphased) Analysis of Two Crude Oils, Analyzed by Unsegmented and Segmented Two Term Mass Calibration Equations

	mass calibration equation	absorption mode	peaks detected	peaks assigned	rms mass error (ppb)
heavy vacuum gas oil	$m/z = A/f + B/f^2$	no	12 211	9 878	101
	$m/z = A_i/f + B_i/f^2$	no	12 211	10 196	76
	$m/z = A/f + B/f^2$	yes	12 215	9 906	110
	$m/z = A_i/f + B_i/f^2$	yes	12 215	10 738	53
North American crude oil	$m/z = A/f + B/f^2$	no	15 117	10 896	199
	$m/z = A_i/f + B_i/f^2$	no	15 117	11 171	138
	$m/z = A/f + B/f^2$	yes	15 177	11 500	202
	$m/z = A_i/f + B_i/f^2$	yes	15 177	13 672	71

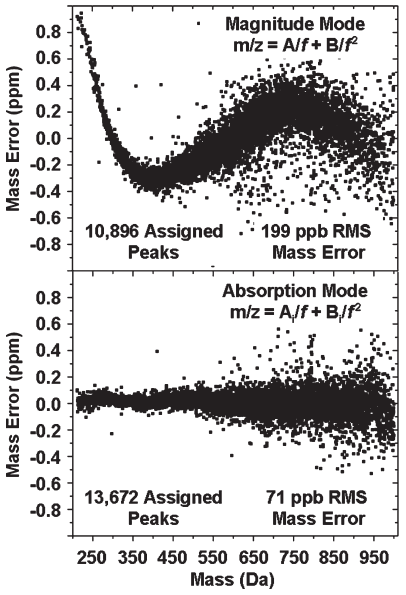

Figure 3. Mass error for electrosprayed negative-ion FTICR mass spectrum of a North American crude oil as a function of m/z. Top: magnitude-mode with unsegmented two term mass calibration. Bottom: absorption-mode with a two term walking calibration.

ion 9.4 T FTICR magnitude and absorption spectra from the HVGO data of Figure 1 and a North American crude oil. The results (magnitude- and absorption-mode) span a spectral abundance range of approximately 190:1 and 430:1 for the North American crude oil and the HVGO. For both samples, the walking calibration significantly reduced rms mass error for both magnitude- and absorption-mode data analysis. The best mass accuracy was obtained for the absorption-mode due to significantly smaller random error. With the combination of walking calibration and absorption-mode data analysis, the rms mass error dropped from ~200 to ~70 ppb for the North American crude oil and from ~100 to ~50 ppb for the HVGO. Figure 3 graphically documents the overall reduction in mass measurement error for the North American crude oil.

Table 2 also reveals an increase in the number of assigned peaks on application of absorption rather than magnitude analysis and/or a walking calibration rather than unsegmented calibration. The increase is due in part to the intrinsically higher resolving power and thus more resolved resonances for absorption mode. Other factors that strongly contribute to the number of assigned peaks are the accuracy with which peaks can be sorted into a given homologous series and a specific series assigned to a unique header atom composition. The systematic error shown in Figure 3 (top) limits the confidence with which our analysis software can perform either of those tasks. Figure 3 (bottom) demonstrates that with a walking calibration and absorption-mode representation both random and m/z-dependent systematic errors are greatly reduced and more peaks can be assigned within a given allowable assignment error. For the samples presented in Table 2, ~90% of the above-threshold peaks could be assigned for absorption-mode with a walking calibration. We believe that the unassigned peaks are mainly spectral noise along with isotopomers composed of more than two heavy isotopes.

CONCLUSIONS

The precision and accuracy of the frequency-to-m/z conversion required to analyze organic mixtures as complex as petroleum crude oil can be improved by a walking calibration, an abundance-dependent term in the calibration equation, and spectral phase correction. Overall, we can reduce rms mass error by as much as 3-fold for electrospray ionization FTICR MS of a distillate fraction from an Athabasca bitumen HVGO and a North American crude oil. Implementation of these techniques also increases the number of assigned peaks by as much as 25%. The improvement in mass accuracy makes automated mass analysis of complex mixtures more accurate and efficient. Addition of an abundance-dependent term to the walking calibration equation and ^{13}C isotopomers to the calibration series was also advantageous. Robust automation of this procedure is currently in progress and should accelerate confident assignment of unique elemental compositions. The use of several calibration series with the same heteroatom composition but different double bond equivalents is also under investigation to extend the calibration mass range. Finally, although we applied the present methods to crude oil FTICR mass spectra, the procedure is general and could be applied to any mass analyzer and any complex mixture with abundant internal calibrants.

AUTHOR INFORMATION

Corresponding Author

*Phone: +1 850 644 0529 (A.G.M.); +1 850 644 0711 (C.L.H.). Fax: +1 850 644 1366 (A.G.M. and C.L.H.). E-mail: marshall@magnet.fsu.edu (A.G.M.); hendrick@magnet.fsu.edu (C.L.H.).

■ ACKNOWLEDGMENT

The authors thank John P. Quinn for help with operation and maintenance of the instrumentation. This work was supported by NSF Division of Materials Research through Grant DMR-0654118 and the State of Florida.

■ REFERENCES

(1) Marshall, A. G.; Hendrickson, C. L.; Jackson, G. S. *Mass Spectrom. Rev.* **1998**, *17*, 1–35.
(2) Shi, W.; Redshaw, M.; Myers, E. G. *Phys. Rev. A* **2005**, *72*, 022510/022511–022510/022518.
(3) Ledford, E. B.; Rempel, D. L.; Gross, M. L. *Anal. Chem.* **1984**, *56*, 2744–2748.
(4) Shi, S. D.-H.; Drader, J. J.; Freitas, M. A.; Hendrickson, C. L.; Marshall, A. G. *Int. J. Mass Spectrom.* **2000**, *195/196*, 591–598.
(5) Leach, F. E., III; Kharchenko, A.; Heeren, R. M. A.; Nikolaev, E. N.; Amster, I. J. *J. Am. Soc. Mass Spectrom.* **2010**, *21*, 203–208.
(6) Xiang, X.; Grosshans, P. B.; Marshall, A. G. *Int. J. Mass Spectrom. Ion Processes* **1993**, *125*, 33–43.
(7) Guan, S.; Gorshkov, M. V.; Alber, G. M.; Marshall, A. G. *Phys. Rev. A* **1993**, *47*, 2730.
(8) Easterling, M. L.; Mize, T. H.; Amster, I. J. *Anal. Chem.* **1999**, *71*, 624–632.
(9) Jeffries, J. B.; Barlow, S. E.; Dunn, G. H. *Int. J. Mass Spectrom. Ion Processes* **1983**, *54*, 169–187.
(10) Muddiman, D. C.; Oberg, A. L. *Anal. Chem.* **2005**, *77*, 2406–2414.
(11) Syka, J. E. P.; Marto, J. A.; Bai, D. L.; Horning, S.; Senko, M. W.; Schwartz, J. C.; Ueberheide, B.; Garcia, B.; Busby, S.; Muratore, T.; Shabanowitz, J.; Hunt, D. F. *J. Proteome Res.* **2004**, *3*, 621–626.
(12) Williams, D. K., Jr.; Muddiman, D. C. *Anal. Chem.* **2007**, *79*, 5058–5063.
(13) Bruce, J. E.; Anderson, G. A.; Brands, M. D.; Pasa-Tolic, L.; Smith, R. D. *J. Am. Soc. Mass Spectrom.* **2000**, *11*, 416–421.
(14) Wu, S.; Kaiser, N. K.; Meng, D.; Anderson, G. A.; Zhang, K.; Bruce, J. E. *J. Proteome Res.* **2005**, *4*, 1434–1441.
(15) Smith, M. J. C. *Abstract of Papers*, 2nd Sanibel Conference on Ion Trapping in Mass Spectrometry, American Society for Mass Spectrometry, Sanibel Island, FL, January 1990.
(16) Masselon, C.; Tolmachev, A. V.; Anderson, G. A.; Harkewicz, R.; Smith, R. D. *J. Am. Soc. Mass Spectrom.* **2002**, *13*, 99–106.
(17) Mitchell, D. W.; Smith, R. D. *Phys. Rev. E* **1995**, *52*, 4366.
(18) Wang, M.; Marshall, A. G. *Int. J. Mass Spectrom. Ion Processes* **1988**, *86*, 31–51.
(19) Rodgers, R. P.; White, F. M.; McIntosh, D. G.; Marshall, A. G. *Rev. Sci. Instrum.* **1998**, *69*, 2278–2284.
(20) Tolmachev, A. V.; Monroe, M. E.; Jaitly, N.; Petyuk, V. A.; Adkins, J. N.; Smith, R. D. *Anal. Chem.* **2006**, *78*, 8374–8385.
(21) Kaiser, N. K.; Quinn, J. P.; Hendrickson, C. L.; Marshall, A. G. *Abstract of Papers*, Proceeding of the 57th Conference on Mass Spectrometry and Allied Topics, American Society for Mass Spectrometry, Philadelphia, PA, May 31—June 4, 2009.
(22) Emmett, M. R.; White, F. M.; Hendrickson, C. L.; Shi, S. D. H.; Marshall, A. G. *J. Am. Soc. Mass Spectrom.* **1998**, *9*, 333–340.
(23) Tolmachev, A. V.; Robinson, E. W.; Wu, S.; Kang, H.; Lourette, N. M.; Pasa-Tolic, L.; Smith, R. D. *J. Am. Soc. Mass Spectrom.* **2008**, *19*, 586–597.
(24) Xian, F.; Hendrickson, C. L.; Blakney, G. T.; Beu, S. C.; Marshall, A. G. *Anal. Chem.* **2010**, *82*, 8807–8812.
(25) Marshall, A. G.; Verdun, F. R. *Fourier Transforms in NMR, Optical, and Mass Spectrometry*; Elsevier Science & Technology: Amsterdam, The Netherlands, 1990.
(26) Hughey, C. A.; Hendrickson, C. L.; Rodgers, R. P.; Marshall, A. G.; Qian, K. *Anal. Chem.* **2001**, *73*, 4676–4681.
(27) Kendrick, E. *Anal. Chem.* **1963**, *35*, 2146–2154.
(28) Blakney, G. T.; Hendrickson, C. L.; Marshall, A. G. *Abstract of Papers*, 55th Conference on Mass Spectrometry and Allied Topics, American Society for Mass Spectrometry, Indianapolis, IN, June 3—7, 2007.